

Critical Temperature of Bose-Einstein Condensation of Hard-Sphere Gases

Peter Grüter and David Ceperley*

Department of Physics, University of Illinois, 1110 West Green Street, Urbana, Illinois 61801

Frank Lalöe†

Laboratoire Kastler Brossel, Ecole Normale Supérieure, 24 rue Lhomond, F-75005 Paris, France

(Received 11 July 1997)

We determine the critical temperature of a 3D homogeneous system of hard-sphere bosons by path-integral Monte Carlo simulations and finite-size scaling. In the low density limit, we find that the critical temperature is increased by the repulsive interactions, as $\Delta T_C/T_0 \sim (na^3)^\gamma$, where $\gamma = 0.34 \pm 0.03$. At high densities the result for liquid helium, namely, a lower critical temperature than in the noninteracting case, is recovered. We give a microscopic explanation for the observed behavior. [S0031-9007(97)04438-4]

PACS numbers: 03.75.Fi, 02.70.Lq, 05.30.Jp

The observation of Bose-Einstein condensation in atomic vapors [1], at temperatures of a few hundreds of nK by evaporative cooling, has revived interest in the theoretical investigation of this phenomenon. In this Letter we study hard-sphere bosons of diameter a confined in a cubic box of volume L^3 . The hard-sphere diameter a corresponds to the s -wave scattering length of a real interatomic potential in a model which is valid at low densities and even yields reasonable results for relatively dense systems such as liquid helium [2].

We determine the critical temperature T_C of this system for various number densities n and compare it to the critical temperature T_0 of the ideal gas [3]. The literature provides contradictory results stemming from analytical studies, even with regard to the sign of $\Delta T_C = T_C - T_0$: A negative sign is predicted by Hartree-Fock theory [4], and a renormalization group (RG) calculation [5]; higher critical temperatures, but with different low density asymptotic behaviors, were the result of Ref. [6], $\Delta T_C/T_0 \sim (na^3)^{1/2}$, Ref. [7], $\Delta T_C/T_0 \sim (na^3)^{1/3}$, and a recent renormalization group calculation [8], which goes beyond the one-loop expansion of Ref. [5], and for which approximately $\Delta T_C/T_0 \sim (na^3)^{1/6}$ [9].

We have used a path-integral Monte Carlo method to obtain our results. In 3D Bose systems both superfluidity and Bose-Einstein condensation are believed to occur at the same critical temperature. We determine this transition temperature by making use of the scaling properties of the superfluid fraction ρ_s/ρ [10,11]. From the hypothesis that close to the bulk transition point thermodynamic quantities in finite systems depend on temperature only through the ratio of a characteristic system size L in our case and the bulk correlation length $\xi(t)$, the following scaling form can be obtained:

$$\rho_s/\rho(t) = L^{-\varphi/\nu} Q(L/\xi(t)), \quad (1)$$

with

$$t = \frac{T - T_C}{T_C} \ll 1. \quad (2)$$

In Eq. (1), $Q(L/\xi(t))$ is an analytic function of ρ_s/ρ for finite L . φ and $-\nu$ are the bulk critical exponents of the superfluid fraction and the correlation length, respectively; their ratio has been measured in helium [12] and calculated with renormalization group techniques [13]; the results are consistent with $\varphi = \nu$. At the transition point the correlation length diverges, so that $Q(L/\xi(t))$ becomes independent of L . This feature allows us to deduce the transition point for the infinite system from simulations of finite-size samples: curves of the scaled superfluid fraction $L\rho_s/\rho(t)$ obtained from different sized systems will intersect at $t = 0$.

In our path-integral Monte Carlo simulation we measure the “stiffness” of the system against twisting the phase of the wave function, when a particle is displaced across the periodic boundary conditions, by means of the winding number distribution. From that we deduce the superfluid fraction [14]. We use the high-temperature approximation for the hard-sphere propagator derived in Ref. [15]. Typically five time-slices were used for the calculations near T_C . (We found that the use of the “image propagator” [16] converged much slower at low density.)

Figure 1 shows the scaled quantity

$$N^{1/3} \rho_s/\rho(T) \quad (3)$$

as a function of temperature for four different particle numbers $N = 27, 64, 125, \text{ and } 216$. Here the dimensionless $N^{1/3}$ has replaced the length L .

Equation (1) implies that the four graphs should intersect at the transition point. However, because of the statistical noise in our data, an accurate estimate of this point is difficult. (The same reason prevented us from using for an estimator the scaled twist free energy as in Ref. [11].) Since $N^{1/3} \rho_s/\rho$ is analytic, we fit our values of this quantity (for 4 values of N and 10 different temperatures close to the transition point) to a function of the form

$$Q(L/\xi(T))|_{T \rightarrow T_C} = Q(0) + qN^{1/(3\nu)}(T - T_C)/T_C, \quad (4)$$

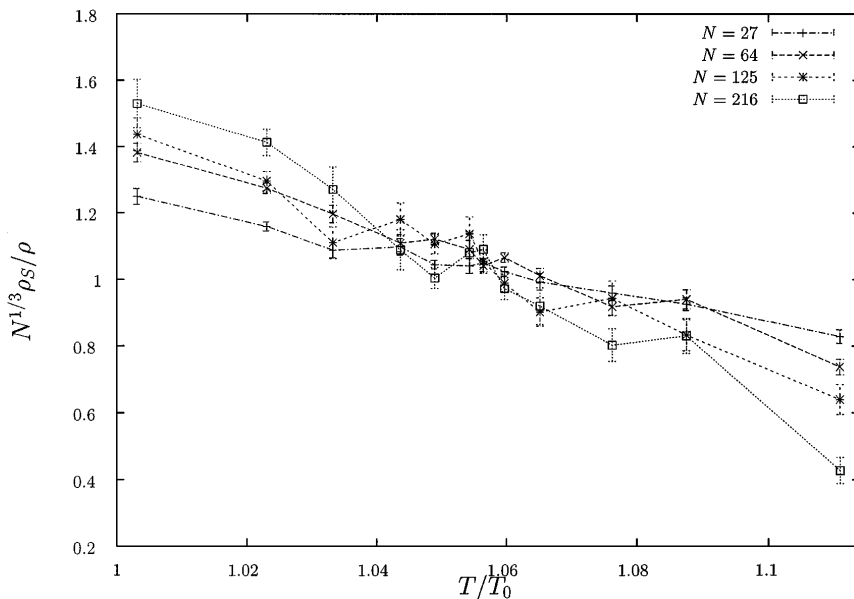


FIG. 1. Scaled superfluid fraction $N^{1/3} \rho_s / \rho$ in function of temperature T as determined by our simulations for $na^3 = 5 \times 10^{-3}$ and $N = 27, 64, 125,$ and 216 . T_0 is the critical temperature of the noninteracting system. The temperature where the four lines are crossing is to be identified with the critical temperature. A quantitative estimate for this temperature is obtained by fitting the values for every N with a straight line and determining the point of intersection for the fitted curves.

and determine the parameters $Q(0)$, q , ν , and T_C . In this way we obtain a quantitative estimate for T_C . Furthermore, we can check the results by comparing our values for $Q(0)$ and the critical exponent ν to results obtained elsewhere. Assuming that the interacting Bose gas falls into the same universality class as the XY model, we expect that

$$\frac{T_0}{T_C} \frac{\zeta(\frac{3}{2})^{2/3}}{2\pi} Q(0) = \text{universal constant.} \quad (5)$$

We find values between 0.29 and 0.33 for the system densities we considered. This is different from the value of 0.49 ± 0.01 obtained in [17]. For the critical exponent of the correlation length, our calculations yield an estimate $-\nu = -0.68 \pm 0.28$, which is in agreement with analytical results [18] and simulations [19] for the 3D XY model, as well as experimental data which give $-\nu = -0.67$. As a matter of fact, the values for T_C depend only slightly on ν : Results obtained with ν fixed to the experimental value differ at most about 0.2% from the ones obtained with letting ν be a free parameter. Figure 2 shows a typical fit.

Figure 3 shows the results of our calculations, the relative change of the critical temperature as a function of the density. We distinguish two regimes: At low densities the critical temperature for the interacting gas is *higher* than that for the noninteracting system. With increasing density the critical temperature attains a broad maximum (near $na^3 \approx 0.01$) before decreasing and coming to its minimum value for the highest densities we have used in our simulations. For comparison, we include in our diagram higher densities experimental and simulation results obtained for liquid helium [11,20]. This system is well described by a hard-sphere model with an effective hard-sphere diameter of $a = 2.2033 \text{ \AA}$ [21]. Superfluid helium exists only for a limited range of densities before it freezes at a density of $na^3 \approx 0.24$ [2].

We have fit the change in transition temperature for densities $5 \times 10^{-6} \leq na^3 \leq 5 \times 10^{-3}$ with

$$\frac{\Delta T_C}{T_0} = c_0 (na^3)^\gamma, \quad (6)$$

and obtained $c_0 = 0.34 \pm 0.06$ and $\gamma = 0.34 \pm 0.03$. Assuming $\gamma = \frac{1}{3}$, the enhancement of T_C is linear in the scattering length a . This exponent is also the result of the analytical study in Ref. [7], which yields, however, a value of c_0 which is about 14 times larger. When mass renormalization is included, it is possible that the RG calculation in Ref. [8] may also yield this exponent [9].

In order to understand our findings on a microscopic level, recall the Feynman picture of superfluidity [22]. The partition function Z of the system can be written as a sum over all states accessible to distinguishable particles:

$$Z = \text{Tr}_{\text{Boltzmann states}} \{S e^{-\beta \mathcal{H}}\}, \quad (7)$$

where S symmetrizes with respect to the particle labels. We can expand the symmetrizer S into a sum over exchange cycles. At high temperatures the only significant contribution comes from the identity operator (cycle length 1) and Z reduces to the partition function for a classical system. At lower and lower temperatures, however, the importance of the contribution of exchange cycles of macroscopic length grows. The statistical correlations extend over longer and longer distances, until—at the transition point—a macroscopic structure, identified as superfluid component, is established.

A necessary condition for these exchange cycles to appear is that the particles must be close together (separated by distances of the order of the thermal wavelength $\lambda_T = 2\pi \hbar^2 / mk_B T$). In an ideal gas, spatial density fluctuations are important, and particle clusters are likely to appear. This creates regions of lower density at other places in the system, which obstruct the formation of macroscopic exchange cycles. On the other hand, in the case of a moderately dense interacting gas, the particles tend to be more homogeneously distributed throughout the whole volume of the system. Analogously to a percolation problem,

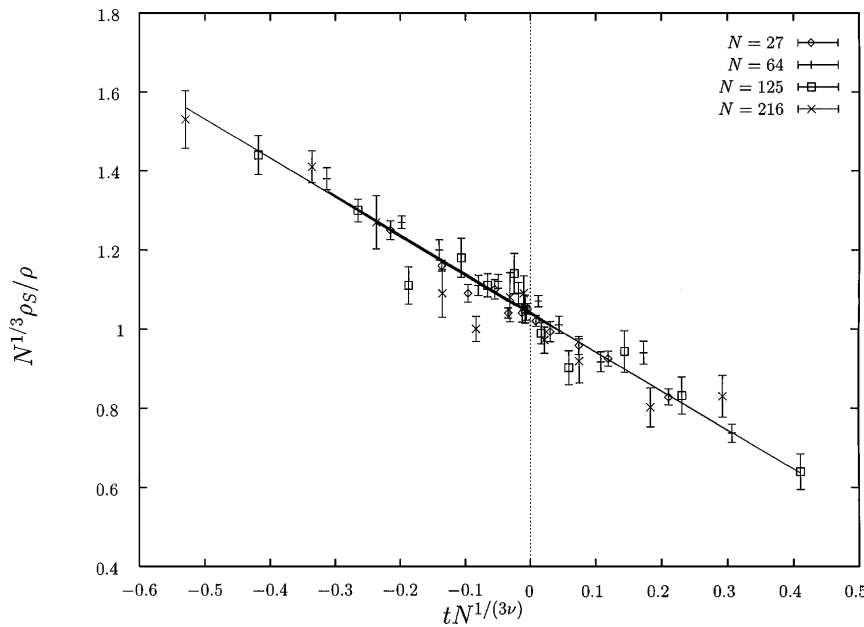


FIG. 2. Result of our fit to the data from Fig. 1. $t = (T - T_C)/T_C$; T_C is the critical temperature for the interacting system and $-\nu$ is the critical exponent of the correlation length, both as obtained by our fit. We find a critical temperature of $T_C/T_0 = 1.057 \pm 0.002$.

it is more likely for every atom to find a neighbor at a suitable distance if there is a repulsive potential, so that the exchange cycles can more easily propagate from one region to the next. Superfluidity is hence “easier” to achieve, meaning that it can occur at higher temperatures.

In order to quantify this understanding of the shift of the critical temperature, we have determined the two-body distribution function $g(r)$. In Fig. 4 we have plotted $g(r)$ for different densities at the bulk superfluid transition temperature for a system of 125 particles. It can be seen that at higher densities the “exchange bump” of the ideal gas decreases and, because of the hard-sphere boundary condition, the distribution tends to become homogeneous. Another way to see that the interactions suppress the spatial density fluctuations is to integrate $g(r)$ over subvolumes of the simulation cell which gives the fluctuation of the

particle number in these subvolumes [23]. We find that the number of particles in subspheres of radius comparable to λ_T fluctuates about 30% more in the case of an ideal gas than for an interacting gas of density $5 \times 10^{-2} a^{-3}$.

At higher densities the atoms cannot exchange with each other without dragging other particles along. The effective mass becomes greater than unity, and the critical temperature is decreased as $T_C \sim 1/m^*$ [4,22].

The results obtained in our case of an isotropic system are different from the ones obtained in a harmonic external potential [24,25], where the repulsive interactions decrease the critical temperature at low densities. In a trap, interactions give rise to two competing effects. The critical temperature is increased by the suppression of density fluctuations (even if those are already smaller than in the isotropic case because of the confinement).

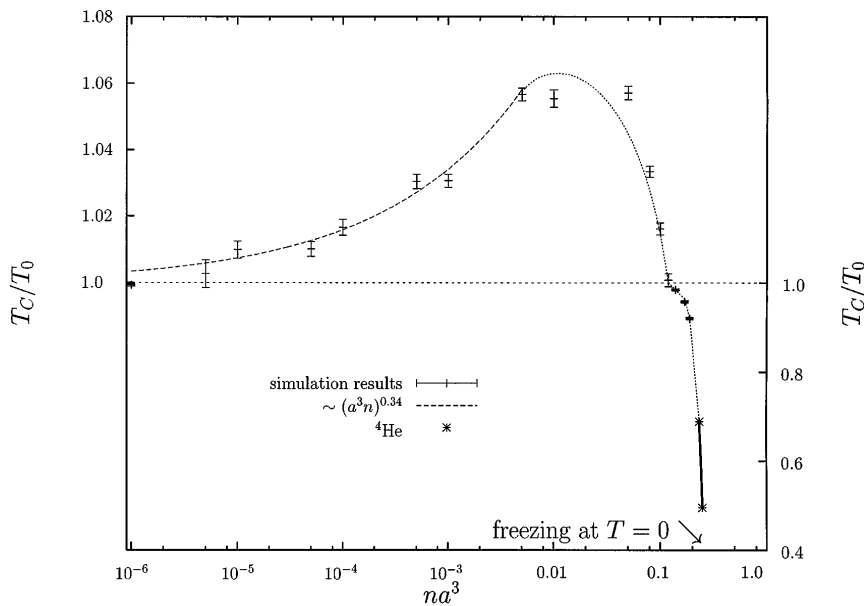


FIG. 3. Critical temperature T_C of an interacting Bose gas versus density: a is the hard-sphere diameter and T_0 is the critical temperature of the noninteracting gas. Two different scales are used for the vertical axis: For temperatures above T_0 the left scale applies and for values below T_0 the right scale applies. For comparison, experimental and simulation results [11,20] obtained for helium (at densities $na^3 = 0.235$ and 0.25) are also included. The dashed curve at low densities presents a fit of the data points between $na^3 = 5 \times 10^{-6}$ and 5×10^{-3} to $1 + c_0(na^3)^\gamma$, yielding $\gamma = 0.34$, the dotted curve is a guide to the eye (note the change of scale at $T_C = T_0$). At zero temperature the hard-sphere system freezes at a density of about $na^3 = 0.25$ [2].

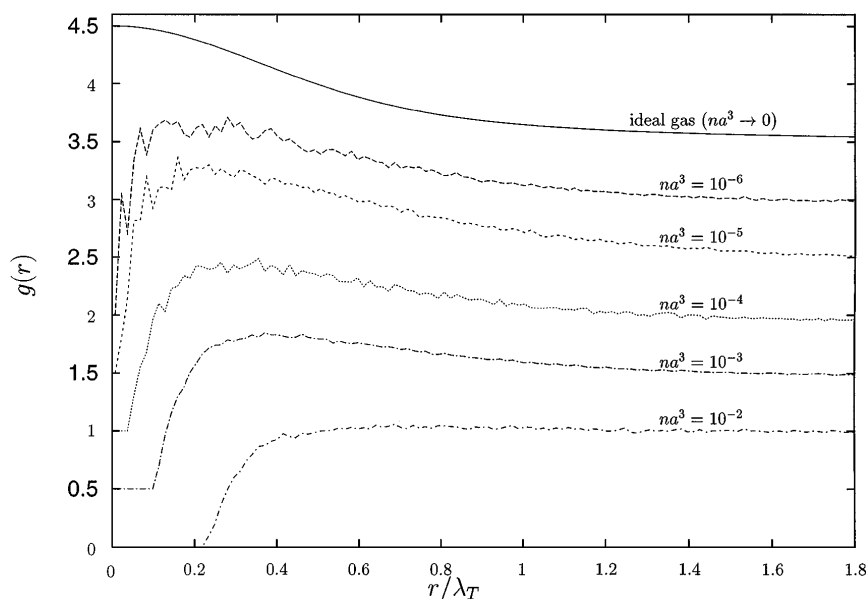


FIG. 4. Two-body distribution function $g(r)$ versus particle distance r in units of the thermal wavelength λ_T for different densities na^3 at the bulk critical temperature. For the sake of visibility, the single curves are shifted vertically by 0.5. The hard-sphere boundary condition changes the short-distance ($r \rightarrow 0$) behavior dramatically. However, for the “percolation-like” theory of superfluidity, the behavior for $r \approx \lambda_T$ is more important, and here the functions for the ideal and the low density gas both feature the appearance of the “exchange bump” for $r \lesssim \lambda_T$: In the non-interacting gas or gases of lower density, many particles cluster together at distances less than the thermal wavelength. In a denser system the interactions are compensating this statistical attraction and the particles fill the system volume homogeneously. This allows for superfluidity to appear at higher temperatures.

On the other hand, the central density is lowered as the condensate wave function is broadened. Both terms are linear in the scattering length; hence, whether T_C is suppressed or increased depends on details of the system such as the number of particles, the trapping frequency ω , and the particle mass [26].

To conclude, the effect of repulsive interactions is different for low and high densities: At low densities, the “density homogenization” effect prevails so that T_C is increased; at high densities, the exchange motion of the atoms—which are behind the Bose-Einstein condensation phenomenon—are hindered by the hard cores so that the critical temperature is decreased. Since, in the experiments on alkali gases, the value of na^3 in the center of the trap does not exceed 10^{-5} , the shifts in T_C remain small (about 1%), but may be observable in larger traps.

The authors thank M. Dewing and W. Krauth for helpful comments and discussions. This project was supported by ONR Grant No. N00014-90-J-1783 and the Department of Physics at the University of Illinois Urbana-Champaign. The computations were performed at the National Center for Supercomputing Applications. The Laboratoire Kastler Brossel is “laboratoire associé au CNRS et à l’Université Paris VI.”

*Electronic address: ceperley@uiuc.edu

†Electronic address: laloe@physique.ens.fr

- [1] E. A. Cornell *et al.*, *Science* **269**, 198 (1995); K. B. Davis *et al.*, *Phys. Rev. Lett.* **75**, 3969 (1995); C. C. Bradley, C. A. Sackett, and R. G. Hulet, *Phys. Rev. Lett.* **78**, 985 (1997).
- [2] M. H. Kalos, D. Levesque, and L. Verlet, *Phys. Rev. A* **9**, 2178 (1974).
- [3] $T_0 = (\hbar^2 2\pi / mk_B) [n / \zeta(\frac{3}{2})]^{2/3}$, where m is the particle mass, k_B is the Boltzmann constant, and $\zeta(\frac{3}{2}) \approx 2.612$.
- [4] A. L. Fetter and J. D. Walecka, *Quantum Theory of Many-Particle System* (McGraw-Hill, New York, 1971).

- [5] T. Toyoda, *Ann. Phys. (N.Y.)* **141**, 154 (1982).
- [6] K. Huang, in *Studies in Statistical Mechanics* (North-Holland, Amsterdam, 1964), Vol. II.
- [7] H. T. C. Stoof, *Phys. Rev. A* **45**, 8398 (1992).
- [8] M. Bijlsma and H. T. C. Stoof, *Phys. Rev. A* **54**, 5085 (1996).
- [9] Unpublished results for the limit $a \rightarrow 0$ according to H. T. C. Stoof gives an exponent very close to $\frac{1}{5}$, in agreement with our calculation.
- [10] M. N. Barber, in *Phase Transitions and Critical Phenomena* (Academic Press, London, 1983), Vol. 8, pp. 146–266.
- [11] E. L. Pollock and K. J. Runge, *Phys. Rev. B* **46**, 3535 (1992).
- [12] G. Ahlers and D. S. Grewall, *Phys. Rev. A* **7**, 2145 (1973).
- [13] C. Le Guillou and J. Zinn-Justin, *Phys. Rev. Lett.* **39**, 95 (1977).
- [14] E. L. Pollock and D. M. Ceperley, *Phys. Rev. B* **36**, 8343 (1987); D. M. Ceperley, *Rev. Mod. Phys.* **67**, 279 (1995).
- [15] J. Cao and B. J. Berne, *J. Chem. Phys.* **97**, 2382 (1992).
- [16] G. Jacucci and E. Omerti, *J. Chem. Phys.* **76**, 3051 (1983).
- [17] M.-C. Cha *et al.*, *Phys. Rev. B* **44**, 6883 (1991).
- [18] C. Le Guillou and J. Zinn-Justin, *Phys. Rev. B* **21**, 3976 (1980).
- [19] Y.-H. Li and S. Teitel, *Phys. Rev. B* **40**, 9122 (1989).
- [20] J. Wilks, *The Properties of Liquid and Solid Helium* (Clarendon Press, Oxford, 1967).
- [21] K. J. Runge and G. V. Chester, *Phys. Rev. B* **38**, 135 (1988).
- [22] R. P. Feynman, *Phys. Rev.* **90**, 1116 (1953); **91**, 1291 (1953).
- [23] R. K. Pathria, *Statistical Mechanics* (Butterworth-Heinemann, Oxford, 1996), 2nd ed., Sect. 14.3.
- [24] S. Giorgini, L. Pitaevskii, and S. Stringari, *Phys. Rev. A* **54**, R4633 (1996).
- [25] W. Krauth, *Phys. Rev. Lett.* **77**, 3695 (1996).
- [26] M. Houbiers, H. T. C. Stoof, and E. A. Cornell, cond-mat/9612198, however, find that in the framework of the results of [8] the critical temperature always decreases with the scattering length.